Am J Transl Res 2024;16(4):1062-1080
www.ajtr.org /ISSN:1943-8141/AJTR0149193

Original Article

Comprehensive analysis of ETS1 expression and its prognostic value in clear cell renal cell carcinoma

Mengying Mo[1], Qiqi Zhu[2], Ling Yang[1], Yanhua Deng[1], Yanna Yu[3,4], Zheng Zhou[1]

[1]Dongguan Hospital of Guangzhou University of Chinese Medicine, Dongguan, Guangdong, China; [2]Guangzhou University of Chinese Medicine, Guangzhou, Guangdong, China; [3]The First Affiliated Hospital of Guangzhou University of Chinese Medicine, Guangzhou, Guangdong, China; [4]Guangdong Clinical Research Academy of Chinese Medicine, Guangzhou, Guangdong, China

Received January 17, 2023; Accepted April 11, 2023; Epub April 15, 2024; Published April 30, 2024

Abstract: Background: ETS1, a member of the large ETS domain family of transcription factors, plays a role in the progression of many types of carcinoma. ETS1 expression has been linked to a more favorable prognosis in renal cell carcinoma. The objective of this study was to assess the predictive significance of ETS1 in individuals suffering from clear cell renal cell carcinoma (ccRCC). Methods: The correlation between ETS1 expression and ccRCC was analyzed. Data on ETS1 and clinical information for ccRCC patients were obtained from the Cancer Genome Atlas database and analyzed using R software. Then, we presented validation results using RT-qPCR (quantitative reverse transcription PCR). The receiver operator characteristic (ROC) curves were generated using the pROC software package to determine the cutoff values for ETS1. Additionally, the ImmuneScore, StromalScore, and ESTIMATEScore were calculated using the ESTIMATES algorithm. The connection between ccRCC and ETS1 was investigated using enrichment analysis based on Gene Oncology and the Kyoto Encyclopedia of Genes and Genomes. The tumor immunity estimation resource (TIMER) and the integrated repository portal for tumor-immune system interactions (TISIDB) databases were utilized to analyze the association between ETS1 expression and immune cell infiltration in ccRCC. The impact of ETS1 on the survival of ccRCC patients was evaluated using the PrognoScan database. We evaluated the Tumor Mutation Burden (TMB) value between the two sets of samples with high and low ETS1 expression, as well as the differences in gene mutations between the two groups. Results: The mRNA expression of ETS1 in ccRCC was higher compared to normal tissues. Results showed a significant positive correlation between elevated ETS1 expression levels and improved overall survival (OS), disease-specific survival (DSS), and progression-free survival (PFS), with a $P < 0.05$. Furthermore, high ETS1 expression levels were closely linked to early tumor stage and prolonged survival time. TMB in the ETS1-high expression group was significantly less than that in the ETS1-low expression group. Conclusions: Downregulation of ETS1 expression correlated with poor prognosis and immune infiltration in ccRCC, further suggesting that ETS1 may be a biomarker for better prognosis in ccRCC patients.

Keywords: Biomarker, ETS1, immune infiltration, clear renal cell carcinoma, prognosis

Introduction

According to cancer statistics, renal cell carcinoma (RCC) is a frequently diagnosed solid malignancy [1]. Clear cell renal cell carcinoma (ccRCC) is the most common subtype of RCC, accounting for up to 80% of all primary kidney tumors [2]. Although surgical intervention remains the primary treatment modality for RCC, the 5-year survival rate of RCC patients is approximately 55%, with 20% to 30% of cases developing metastatic cancer after surgery [3, 4]. Furthermore, the biologic behavior of RCC varies widely, ranging from indolent to highly aggressive, resulting in variable therapeutic outcomes [5]. Consequently, there is an urgent need to comprehend RCC tumor biology and investigate prognostic biomarkers for these patients.

ETS 1 is the ancestor of the large family of ETS transcription factors, whose members possess a distinct DNA binding domain [6, 7]. ETS1 is primarily known as a transcriptional activator and is a 54 kDa nuclear protein, though it is also capable of repressing gene transcription [8, 9]. Its vital roles in immunity and pro-angiogenesis have been well established [10-12]. For example, the silencing of EST1 restrained hepatocellular carcinoma (HCC) cell proliferation, invasion and migration, and induced cell apoptosis. The development of HCC may be delayed

https://doi.org/10.62347/QNSV5278

by down-regulating EST1 [12]. However, ETS1 is frequently overexpressed in human cancers and implicated in the MAPK signaling pathway, leading to its characterization as an oncogenic factor [13]. Nevertheless, recent research has demonstrated that ETS1 has a tumor-suppressing function by selectively binding to wild-type p53 and enhancing its tumor-suppressive role [14]. Moreover, a previous study reported that ETS1 was a significant transcriptional repressor of the A3A promoter, indicating that it may have a tumor-suppressing function in ccRCC [15].

ETS1 was identified as a direct downstream target of miR-766 in cells, and these findings indicate that miR-766 may hinder the progression of ccRCC by directly regulating ETS1 [16]. The expression patterns of miR-766 vary among different types of human cancer, and prior research has shown that miR-766 is significantly under-expressed in ccRCC cell lines. The decreased levels of miR-766 expression are linked to the clinical stage of ccRCC, and patients with ccRCC and low miR-766 levels have a poorer prognosis compared to those with high miR-766 levels [17]. Despite this, the comprehensive role of ETS1 in ccRCC remains elusive. Thus, we conducted an investigation into the prognostic role of ETS1 in ccRCC and its association with immunity using data mining from The Cancer Genome Atlas database (TCGA).

Methods

Data acquisition and processing

We downloaded data from the official website of TCGA (https://portal.gdc.cancer.gov/) for several cancers, including ccRCC ETS1 transcriptome data and related clinical information [18]. For each of the 30 cancers analyzed, the normal group consisted of at least five samples. The FPKM-formatted data were initially converted to TPM and $\log_2$ formats for subsequent analysis. We ultimately retained RNA-seq data from 539 ccRCC and 72 adjacent normal tissues, all of which included ETS1 gene expression data and related clinical information such as age, sex, clinical stage, and survival status.

Expression analysis of ETS1

mRNA expression data were reported as mean ± SD. We performed statistical analysis using R software (v4.2.2) (https://www.r-project.org/) and utilized the ggplot2 package to visualize the differences. We evaluated the distinctions between ccRCC and adjacent normal tissues by conducting the paired t and Mann-Whitney U tests. We generated a ROC curve using the pROC software package to determine the cut-off for ETS1 [19]. In this study, UALCAN (http://ualcan.path.uab.edu/) was used to comprehensively analyze ETS1 protein expression [20].

Immunohistochemical staining in HPA database, total protein, or phosphoprotein expression by CPTAC analysis

The Human Protein Atlas (HPA, http://www.proteinatlas.org/) online database was explored to validate the ETS1 protein expression in ccRCC by immunohistochemical staining [21]. We also utilized the UALCAN database (http://ualcan.path.uab.edu/analysis-prot.html) to validate the ETS1 total protein expression between the primary ccRCC tumor and normal tissues by CPTAC analysis [22]. Moreover, ETS1 proteins with phosphorylation sites at the S26 and S251 were also explored to detect differences between the primary tumor and normal tissues [23].

Univariate/multivariate Cox hazard regression analyses and nomogram construction

We performed univariate/multivariate Cox hazard regression using R (version 4.2.2; https://www.r-project.org/) to analyze the independent prognostic factors and clinical characteristics of ccRCC, including age, grade, stage, sex, race, and treatment outcome. To predict the OS probability, we utilized the 'RMS' and 'Survival ROC' packages in R to generate a nomogram, and calculated the area under the curve (AUC) to assess the individual predictors' performance in predicting survival. We evaluated the constructed nomogram's performance through calibration curves and C-indices.

Gene set enrichment analysis (GSEA) and protein-protein interaction and enrichment analysis of ETS1

In order to identify ETS1-related signaling pathways, GSEA was performed to figure out the gene sets displayed statistically significant differences among high-ETS1 groups and low-ETS1 groups, with the consideration of the nor-

malized enrichment score (NES) > 1.5 and nominal *P*-value < 0.05 as the threshold [24]. Each analysis includes at least 1000 times permutation tests to discover significant critical biologic pathways. A protein-protein interaction (PPI) network was constructed using the public database STRING (http://string-db.org) to retrieve the co-expressed genes. Functionally condensed analyses of co-expressed genes were performed using the "Cluster Profiler" R package and visualized using the "ggplot2" R package in Gene Ontology and the Kyoto Encyclopedia of Genes and Genomes [25, 26].

Tumor microenvironment, tumor immune infiltration, immune checkpoint molecules, and immune cell pathways

Based on the TIMER database, the relationship between ETS1 expression in ccRCC and six types of immune-infiltrating cells, including B cells, CD4+ T cells, CD8+ T cells, neutrophils, macrophages, and dendritic cells, was analyzed. TISIDB (http://cis.hku.hk/TISIDB/) was used to explore ETS1 expression in tumor tissues and tumor-infiltrating lymphocytes (TILs) [27]. Following the gene expression profile analysis, we employed gene set variation analysis to assess the TILs' relative abundance. We used Spearman's test to investigate the correlation between ETS1 and TILs. The expression matrix of ETS1 was utilized to compute the ImmuneScore, StromalScore, and ESTIMATEScore through the ESTIMATES algorithm, with a cut-off value of $P < 0.001$ [28]. We also calculated immune cell infiltration in ccRCC using CIBERSORT with $P < 0.001$ as the cutoff value [29]. We conducted these analyses using the 'limma' R package and visualized this using the 'reshape2' and 'RColorBrewer' R packages. The aforementioned analyses were performed using the Sangerbox tools (http://www.sangerbox.com/tool).

Tumor mutational burden

We obtained mutation data of ETS1 from the cBioPortal web platform (https://www.cbioportal.org/). Using a z-score threshold of ± 1.5, we explored the genomic profiles of ETS1 and calculated the TMB as the number of tumor mutations per Mb in each sample, with a TMB threshold of 10 mut/Mb. We then analyzed the relationship between ETS1 expression and TMB. Furthermore, we compared the TMB values of the two groups, with high or low expression of ETS1, and conducted further analysis to determine the differences in gene mutations between the two groups of samples.

Verification of ETS1 by RT-qPCR

Ten pairs of clinical ccRCC samples and adjacent kidney tissues frozen in liquid nitrogen were obtained from primary ccRCC patients undergoing radical nephrectomy at the Department of Urology, The First Affiliated Hospital of Guangzhou University of Chinese Medicine. According to the manufacturer's instructions, total RNA was extracted using TRIzol reagent (Invitrogen, Waltham, MA, USA), cDNA was synthesized and the qRT-PCR was performed and calculated by means of $2^{-\Delta\Delta Ct}$ methods. GAPDH served as an internal standard control for mRNA expression. Related primers were as follows: ETS1, Gene ID: NM_005238.4, F: 5'-GAAGAGTGGTGGGTGGTTTAT-3', R: 5'-CAGATTTGCCCATCCTTCCT-3'; GAPDH, Gene ID: NM_001256799.3, F: 5'-CAAGAGCACAAGAGGAAGAGAG-3', R: 5'-CTACATGGCAACTGTGAGGAG-3'. This study was approved by the Institutional Research Ethics Committees of The First Affiliated Hospital of Guangzhou University of Chinese Medicine.

Results

Relative expression level of ETS1 in ccRCC

To accurately evaluate the expression of ETS1 mRNA in different tumors, we excluded datasets containing less than five samples in the normal group from the analysis. We obtained the expression levels of ETS1 mRNA in 33 different carcinomas from TCGA, as shown in **Figure 1A**. These data demonstrate the aberrant expression of ETS1 mRNA in various cancer types. The boxplot analysis of the TCGA ccRCC dataset revealed a significantly higher expression of ETS1 in ccRCC tumors when compared to normal kidney tissues ($P < 0.001$, Normal = 72 and Tumor = 539, **Figure 1B**). We obtained the same results from pairwise boxplot analysis ($P < 0.001$, Normal = 72 and Tumor = 72, **Figure 1C**). Furthermore, immunohistochemical staining of HPA demonstrated an up-regulation of ETS1 protein expression in ccRCC tissues (**Figure 1D**). These results indicate an up-regulation of both ETS1 mRNA and protein expression in ccRCC tissue.

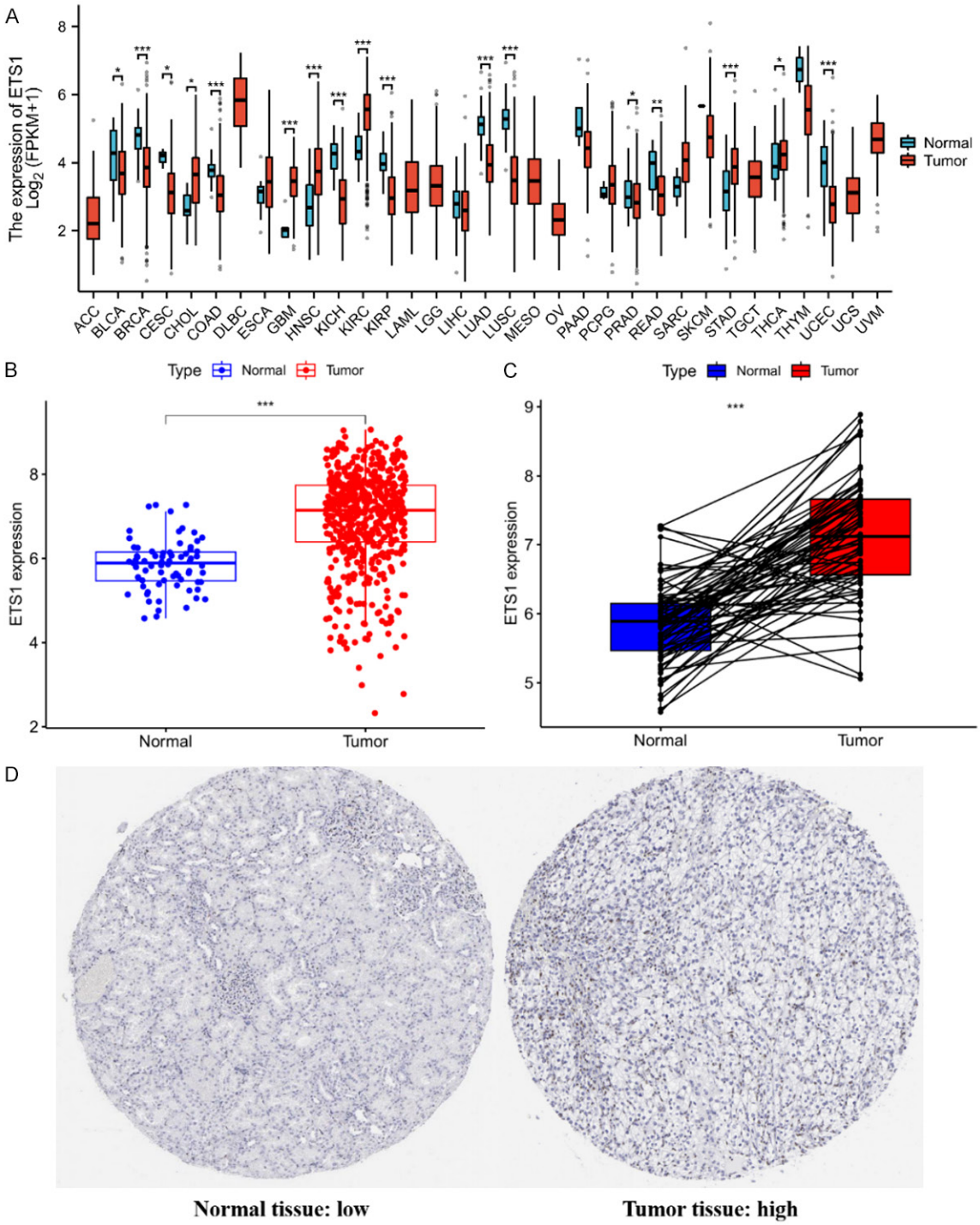

Figure 1. Relative expression level of ETS1 in ccRCC from TCGA and HPA database. A. Relative ETS1 mRNA expression levels in pan-cancers from TCGA database; B. Boxplot of ETS1 expression comparing ccRCC and normal tissues in the TCGA dataset (Normal = 72 and Tumor = 539); C. Pairwise boxplot of ETS1 expression between the ccRCC and normal tissues in TCGA dataset (Normal = 72 and Tumor = 72); D. Immunohistochemical staining (×200) from the HPA database for ETS1 (Antibody: CAB002575; normal tissue: male, age 28, kidney; tumor tissue: female, age 52, kidney). BRCA, breast invasive carcinoma; CHOL, cholangiocarcinoma; COAD, colon adenocarcinoma; ESCA, esophageal carcinoma; GBM, glioblastoma mutiforme; HNSC, head and neck squamous cell carcinoma; KICH, kidney chromophobe; KIRC, kidney renal clear cell carcinoma; KIRP, kidney renal papillary cell carcinoma; LIHC, liver hepatocellular carcinoma; LUAD, lung adenocarcinoma; LUSC, lung squamous cell carcinoma; PRAD, prostate adenocarcinoma; PCPG, pheochromocytoma and paraganglioma; READ, rectum adenocarcinoma; STAD, stomach adenocarcinoma; THCA, thyroid carcinoma; UCEC, uterine corpus endometrial carcinoma; USC, uterine serous carcinoma; UVM, uveal melanoma.

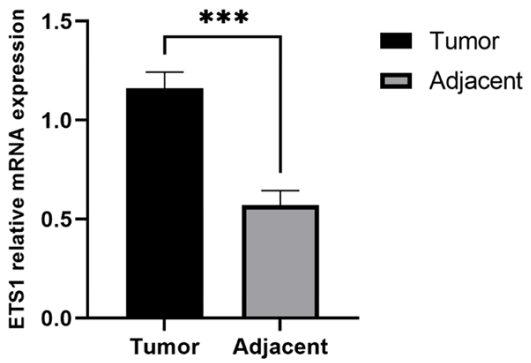

Figure 2. RT-qPCR analysis of ETS1 mRNA expression in 10 pairs of ccRCC tissues and paired adjacent tissues. ccRCC, Clear cell renal cell carcinoma.

Verification of ETS1 by RT-PCR

We utilized qRT-PCR to validate that ETS1 mRNA expression mRNA in 10 pairs of ccRCC tissues was higher than that in adjacent tissues ($P < 0.001$, **Figure 2**).

Total protein or phosphoprotein expression of ETS1 in ccRCC by CPTAC analysis

We validated the expression of total protein and phosphoprotein of ETS1 through CPTAC analysis using the UALCAN website. The results showed that the total protein of ETS1 was significantly overexpressed in primary ccRCC tumors compared to normal kidney tissues ($P < 0.001$), as illustrated in **Figure 3A**. The distribution of ETS1 total protein expression in different grades or stages was shown in **Figure 3B**, **3C**, respectively. With regards to the phosphorylation sites at S26, ETS1 phosphoprotein expression was significantly higher in primary ccRCC tumors than in normal kidney tissues, except for S251 ($P < 0.05$, **Figure 3D**, **3E**).

Relationships between ETS1 mRNA levels and clinicopathologic characteristics of ccRCC patients

ROC curve analysis showed that the AUC value of ETS1 was 0.843 (95% CI: 0.810-0.876) (**Figure 4A**). When the cut-off value was 4.861, the sensitivity, specificity, and accuracy of ETS1 were 89.9%, 75.9%, and 64.87%, respectively. The positive and negative predictive values were 33.0% and 98.1%, respectively. Our analysis showed that ETS1 is a promising biomarker for distinguishing ccRCC tissues from normal tissues. Kaplan-Meier (K-M) survival analysis showed that ccRCC patients in the low-ETS1 groups had a decreased OS compared to those in the high-ETS1 groups ($P < 0.001$, **Figure 4B**).

Table 1 presents the baseline characteristics of ccRCC patients. The relationship between ETS1 mRNA expression and clinicopathologic features was analyzed using the Mann-Whitney U test and logistic regression based on TCGA data. The results in **Table 1** indicate that ETS1 expression level was significantly correlated with gender ($P = 0.009$), pathologic stage ($P < 0.001$), histologic grade ($P < 0.001$), T stage ($P < 0.001$), M stage ($P = 0.007$), serum calcium ($P = 0.007$), OS ($P < 0.001$), disease-free survival (DFS) ($P < 0.001$) and progression free survival (PFS) ($P < 0.001$). **Figure 5A-I** shows that ETS1 expression was higher in patients with earlier pathologic stage (stages I and II versus stages III and IV) and patients without lymph node metastases ($P < 0.05$). Higher expression levels were significantly correlated with better OS, DFS, and PFS ($P < 0.05$). However, no significant correlation was found between ETS1 expression level and other clinicopathologic features such as N stage and age ($P > 0.05$). In conclusion, these results suggest that ETS1 is highly correlated with earlier tumor clinical staging and longer survival time, indicating that ETS1 may serve as a biomarker for better prognosis in ccRCC patients.

Furthermore, Cox univariate and multivariate survival analyses were conducted to evaluate the prognostic significance of ETS1 expression in ccRCC patients. As depicted in **Figure 6** and **Table 2**, high expression of ETS1 ($P < 0.001$) was found to be associated with lower pathologic stage ($P < 0.001$), T stage, and M stage ($P = 0.006$), which is consistent with our previous finding. These findings highlight the use of ETS1 expression as a valuable tool in guiding clinical decision-making and assessing treatment efficacy for patients with ccRCC.

Nomogram construction based on ETS1 and clinicopathologic variables

Based on our nomogram construction, we estimated the survival rates of ccRCC patients at 1, 3, and 5 years, and obtained the total points. Thus, we concluded that the predictive method is more intuitive (**Figure 7A**). The calibration curves of 1-, 3-, and 5-year survival (**Figure**

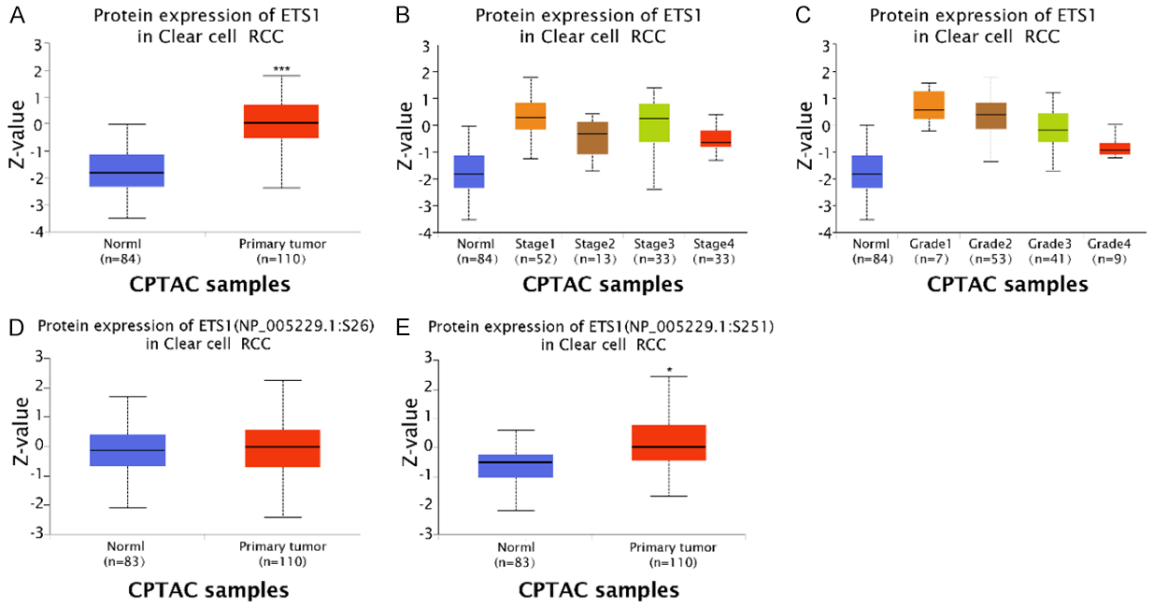

Figure 3. Phosphoprotein expression of ETS1 in ccRCC by CPTAC analysis. A. Total ETS1 protein expression distribution in ccRCC primary tumor and normal tissues; B. Total ETS1 protein expression distribution according to stage; C. Total ETS1 protein expression distribution according to grade; D. Expression of ETS1 phosphoprotein with site at S26 in ccRCC primary tumor and normal tissues; E. Expression of ETS1 phosphoprotein with site at S251 in ccRCC primary tumor and normal tissues. $^{*}P < 0.05$, $^{***}P < 0.001$. ccRCC, Clear cell renal cell carcinoma.

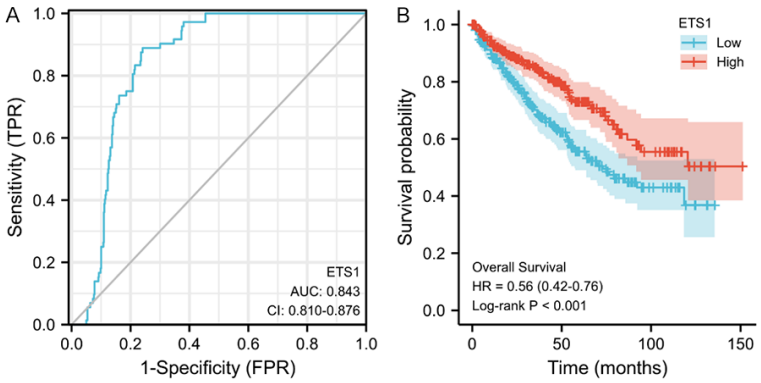

Figure 4. Differential expression and prognostic survival value of ETS1. A. ROC curves and their area under the curve (AUC) for ETS1; B. K-M survival analysis of ETS1.

7B-D) further showed that our nomogram construction was accurate.

ETS1-related co-expressed genome maps and functional annotation analyses

PPI networks and functional annotations were generated using the Gene Ontology string database and the Kyoto Encyclopedia of Genes and Genomes. **Figure 8A** depicts the ETS1 network with ten co-expressed genes. Gene co-expression analyses were performed to explore the correlation between ETS1 expression and related genes in ccRCC patients. As shown in **Figure 8B**, **8C**, ETS1 expression was significantly linked to many related genes expressions, including WWFP1, UBTFL6, APLNR, SH2B3, and GIMAP8. To identify signaling pathways associated with ETS1, we performed GSEA between high and low ETS1 groups, using a nominal $P < 0.05$ and a normalized enrichment score (NES) > 1.5 as the threshold. As shown in **Figure 8D**, we identified two signaling pathways that were significantly enriched in the high ETS1 expression phenotype: chemokine signaling pathway, endocytosis, neurotrophin signaling pathway and small cell lung cancer. To investigate the biologic function of overlapping genes, GO/KEGG analyses were performed by Metascape database. As shown in **Figure 8E**, BP terms were associated with cell migration, including “ameboidal-type cell migration”, “epithelium migration”, “tissue migration”, etc. The

Table 1. Clinical characteristics of ccRCC patients (TCGA)

Characteristic	Low expression of ETS1	High expression of ETS1	*P*
n	269	270	
T stage, n (%)			< 0.001
T1	114 (21.2%)	164 (30.4%)	
T2	45 (8.3%)	26 (4.8%)	
T3	101 (18.7%)	78 (14.5%)	
T4	9 (1.7%)	2 (0.4%)	
N stage, n (%)			0.132
N0	126 (49%)	115 (44.7%)	
N1	12 (4.7%)	4 (1.6%)	
M stage, n (%)			0.007
M0	200 (39.5%)	228 (45.1%)	
M1	50 (9.9%)	28 (5.5%)	
Pathologic stage, n (%)			< 0.001
Stage I	110 (20.5%)	162 (30.2%)	
Stage II	35 (6.5%)	24 (4.5%)	
Stage III	68 (12.7%)	55 (10.3%)	
Stage IV	54 (10.1%)	28 (5.2%)	
Gender, n (%)			0.009
Female	78 (14.5%)	108 (20%)	
Male	191 (35.4%)	162 (30.1%)	
Age, n (%)			0.093
≤ 60	124 (23%)	145 (26.9%)	
> 60	145 (26.9%)	125 (23.2%)	
Histologic grade, n (%)			< 0.001
G1	4 (0.8%)	10 (1.9%)	
G2	93 (17.5%)	142 (26.7%)	
G3	120 (22.6%)	87 (16.4%)	
G4	46 (8.7%)	29 (5.5%)	
Serum calcium, n (%)			0.007
Elevated	7 (1.9%)	3 (0.8%)	
Low	88 (24%)	115 (31.4%)	
Normal	90 (24.6%)	63 (17.2%)	
Hemoglobin, n (%)			0.976
Elevated	3 (0.7%)	2 (0.4%)	
Low	132 (28.8%)	131 (28.5%)	
Normal	97 (21.1%)	94 (20.5%)	
OS event, n (%)			< 0.001
Alive	161 (29.9%)	205 (38%)	
Dead	108 (20%)	65 (12.1%)	
DSS event, n (%)			< 0.001
Alive	187 (35.4%)	233 (44.1%)	
Dead	77 (14.6%)	31 (5.9%)	
PFS event, n (%)			< 0.001
Alive	167 (31%)	211 (39.1%)	
Dead	102 (18.9%)	59 (10.9%)	
Age, median (IQR)	62 (53, 71)	59.5 (51, 69)	0.047

OS, overall survival; DSS, disease-specific survival; PFS, progression-free survival.

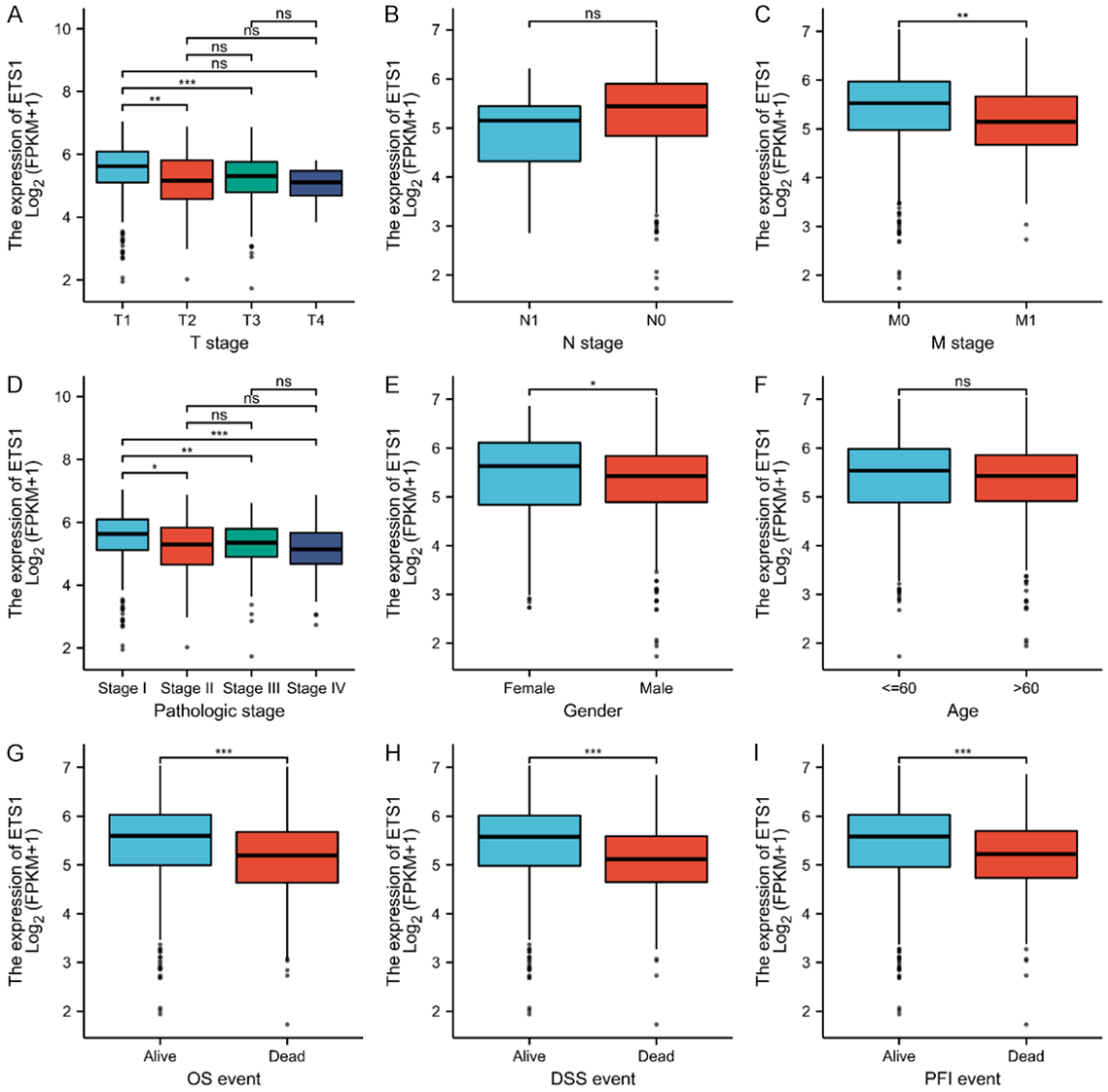

Figure 5. Relationships between ETS1 mRNA levels and clinicopathologic characteristics. OS, overall survival; DSS, disease-specific survival; PFI, progression-free survival.

top 3 CC terms were "apical part of cell", "collagen-containing extracellular matrix" and "apical plasma membrane". The top 3 MF terms were "passive transmembrane transporter activity", "channel activity" and "ion channel activity". The top 30 of enriched sets are listed in **Figure 8F**. An enrichment analysis suggested that ETS1 and its-related partners were functional mediators for neuroactive ligand-receptor interaction, including PI3K-Akt signaling pathway, MAPK signaling pathway, Calcium signaling pathway, Rap1 signaling pathway, and cAMP signaling pathway. These genes are also linked to the inflammatory process, including response to bacteria, tuberculosis, phagocytosis, macrophage activation, and endocytosis.

Analysis of ETS1 and tumor microenvironment, tumor immune infiltration, immune cell pathway, immune checkpoint molecules, and tumor mutation burden in ccRCC

We analyzed tumor immune infiltration, immune cell pathways, and immune checkpoint molecules to explore further any relationship between ETS1 and immunity (**Figure 9**). For TIMER database-related tumor immune infiltration, high levels of ETS1 were significantly associated with B cell, CD8+ T Cell, CD4+ T cell, macrophage, neutrophil, and dendritic cell (all $P < 0.001$, **Figure 9A**). According to the **Figure 9B**, **9C** plot, CD8 T cells, CD4 memory resting T cells, T cells follicular helper, T cells regulatory

A

Characteristics	Total(N)	HR(95% CI) Univariate analysis	P value Univariate analysis
T stage	523		
T1	175	Reference	
T2	282	1.521 (1.068-2.166)	0.02
T3	47	2.937 (1.746-4.941)	<0.001
T4	19	3.326 (1.751-6.316)	<0.001
N stage	167		
N1	94	Reference	
N2	71	1.281 (0.848-1.934)	0.239
N3	2	0.000 (0.000-Inf)	0.995
M stage	377		
M0	352	Reference	
M1	25	2.136 (1.248-3.653)	0.006
Gender	526		
Female	280	Reference	
Male	246	1.070 (0.803-1.426)	0.642
Age	516		
<=65	255	Reference	
>65	261	1.223 (0.916-1.635)	0.172
Pathologic stage	518		
Stage I	290	Reference	
Stage II	121	2.418 (1.691-3.457)	<0.001
Stage III	81	3.544 (2.437-5.154)	<0.001
Stage IV	26	3.790 (2.193-6.548)	<0.001
ETS1	526	1.011 (0.855-1.195)	0.9

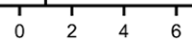

B

Characteristics	Total(N)	HR(95% CI) Multivariate analysis	P value Multivariate analysis
T stage	523		
T1	175		
T2	282	1.606 (1.018-2.532)	0.042
T3	47	2.499 (1.285-4.861)	0.007
T4	19	1.486 (0.692-3.194)	0.31
N stage	167		
N1	94		
N2	71		
N3	2		
M stage	377		
M0	352		
M1	25	3.272 (1.780-6.014)	<0.001
Gender	526		
Female	280		
Male	246		
Age	516		
<=65	255		
>65	261		
Pathologic stage	518		
Stage I	290		
Stage II	121	1.798 (1.158-2.791)	0.009
Stage III	81	3.282 (2.054-5.244)	<0.001
Stage IV	26		
ETS1	526		

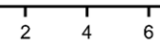

Figure 6. Cox regression analysis of forest map. A. Cox univariate analysis; B. Cox multivariate analysis.

Table 2. Cox regression analysis of clinical prognosis

Characteristic	Total (N)	HR (95% CI)		*P*-value	
		Univariate analysis	Multivariate analysis	Univariate analysis	Multivariate analysis
T stage	523				
T1	175	Reference			
T2	282	1.521 (1.068-2.166)	1.606 (1.018-2.532)	0.02*	0.042*
T3	47	2.937 (1.746-4.941)	2.499 (1.285-4.861)	< 0.001*	0.007*
T4	19	3.326 (1.751-6.316)	1.486 (0.692-3.194)	< 0.001*	0.31
N stage	167				
N1	94	Reference			
N2	71	1.281 (0.848-1.934)		0.239	
N3	2	0.000 (0.000-Inf)		0.995	
M stage	377				
M0	352	Reference			
M1	25	2.136 (1.248-3.653)	3.272 (1.780-6.014)	0.006*	< 0.001*
Gender	526				
Female	280	Reference			
Male	246	1.070 (0.803-1.426)		0.642	
Age	516				
≤ 65	255	Reference			
> 65	261	1.223 (0.916-1.635)		0.172	
Pathologic stage	518				
Stage I	290	Reference			
Stage II	121	2.418 (1.691-3.457)	1.798 (1.158-2.791)	< 0.001*	0.009*
Stage III	81	3.544 (2.437-5.154)	3.282 (2.054-5.244)	< 0.001*	< 0.001*
Stage IV	26	3.790 (2.193-6.548)		< 0.001*	
ETS1	526	1.011 (0.855-1.195)		0.9	

CI, confidence interval; HR, hazard ratio. *$P < 0.05$.

(Tregs), NK cells resting, NK cells activated, Macrophages M0, Macrophages M1, and resting Mast cells, the infiltration levels of the seven kinds of immune cells were significantly different between the high and low expression groups (all $P < 0.05$). Additionally, the TIMER database-related immune checkpoint analysis showed that ETS1 was positively correlated with HAVCR2, CD200R1, and TNFRSF25 ((all R > 0.2, $P < 0.05$); see **Figure 9D**, **9E**).

In terms of tumor microenvironment, ETS1 was markedly related to StromalScore and ESTIMATEScore (both $P < 0.05$, **Figure 10A**); however, it was not linked to ImmuneScore ($P = 0.111$, **Figure 10A**). The above results have confirmed the correlation between the ETS1 gene and stromal cells and immune cells in the immune microenvironment. The expression or copy number variation of ETS1 gene will affect the tumor microenvironment and may play an important role in the occurrence, development, metastasis, and immune response of cancer. To further investigate the relationship between ETS1 and TMB, the TMB value of each patient in TCGA database was calculated, and patients were assigned to a wild-type group or mutation group based on gene mutation statuses. As shown in **Figure 10B**, patients with higher expression of ETS1 showed a lower TMB (R = -0.15, $P < 0.05$).

Discussion

Numerous investigations have validated that ETS1 expression is linked to unfavorable prognosis in most carcinomas [30]. Nonetheless, the operational role of Ets1 protein and the regulatory mechanism for its expression and stability could diverge depending on the specific cellular milieu and tumor tissue category [31]. Herein, we scrutinize the ETS1 expression in both cancerous and normal tissues of ccRCC through the use of the TCGA database.

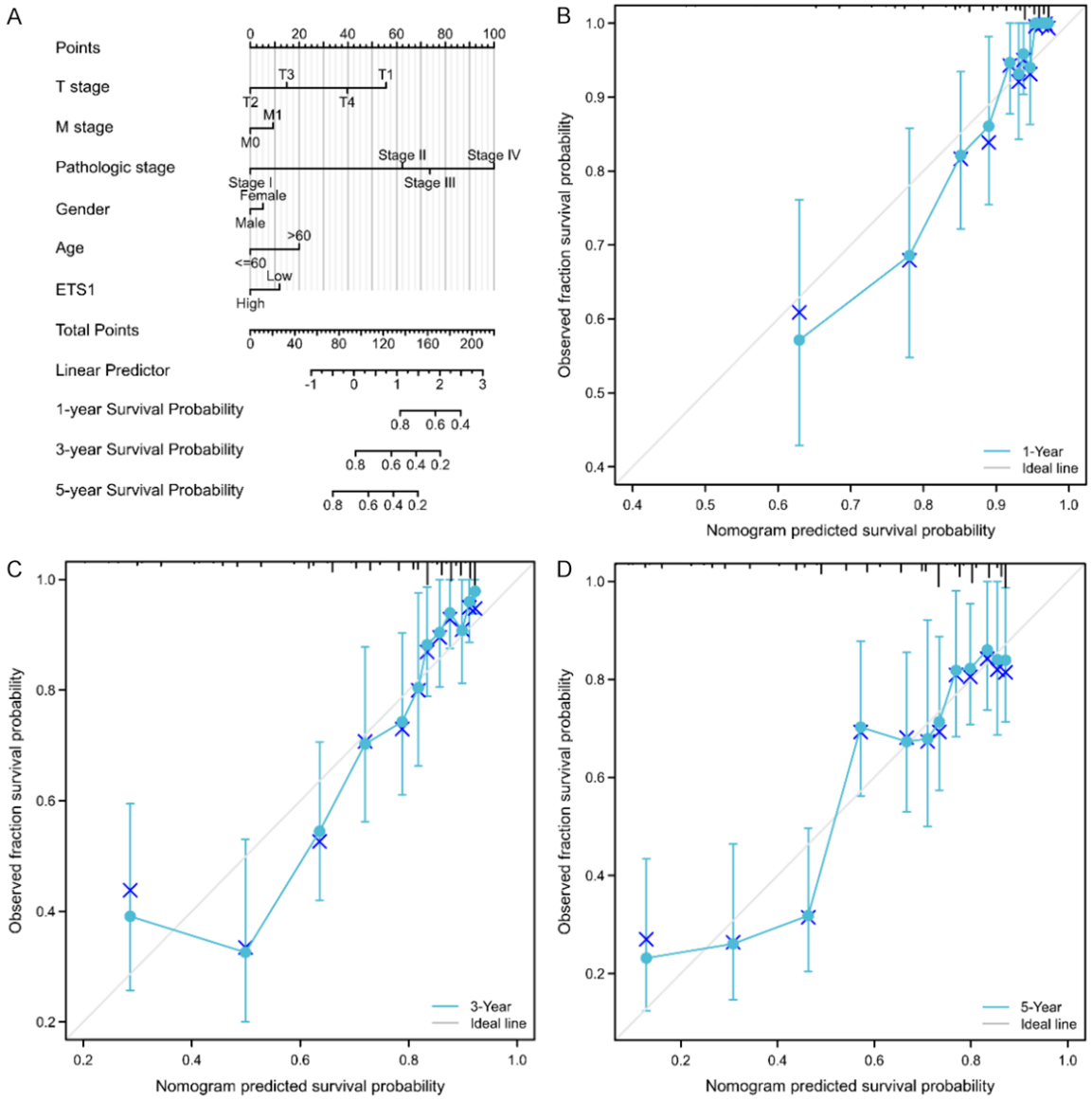

Figure 7. Nomogram construction and evaluation. A. Nomogram construction based on ETS1 and clinicopathologic variables; B. Calibration curves of 1-; C. 3-; D. 5-year survival.

Generally, heightened ETS1 protein or RNA expression in cancerous cells of paraffin-embedded formalin-fixed biopsies has often been correlated with elevated grading, worse differentiation, and/or augmented invasiveness in various carcinomas, such as breast, colorectal, endometrial, esophageal, gastric, hepatocellular, and lung cancer [32, 33]. However, in the case of ccRCC, ETS1 can be a notable transcriptional repressor of the A3A promoter, and may serve as a tumor suppressor. In this study, we have discovered that ETS1 can be utilized as a biomarker to predict a favorable prognosis and extended survival period for ccRCC patients.

In this study, we investigated the correlation between ETS1 expression and the survival of ccRCC patients by performing data mining on TCGA. Our findings demonstrated that ETS1 exhibited greater expression levels in ccRCC tumors than in normal kidney tissues, and this heightened ETS1 expression was associated with a prolonged OS, DFS, and PFS, as well as a moderate degree of diagnostic precision. Moreover, logistic regression analysis revealed that ETS1 exhibited a significant inverse correlation with pathologic stage, histologic grade, T stage, and M stage, which are all indicators of cancer progression. These findings were supported by the results of univariate/multivariate

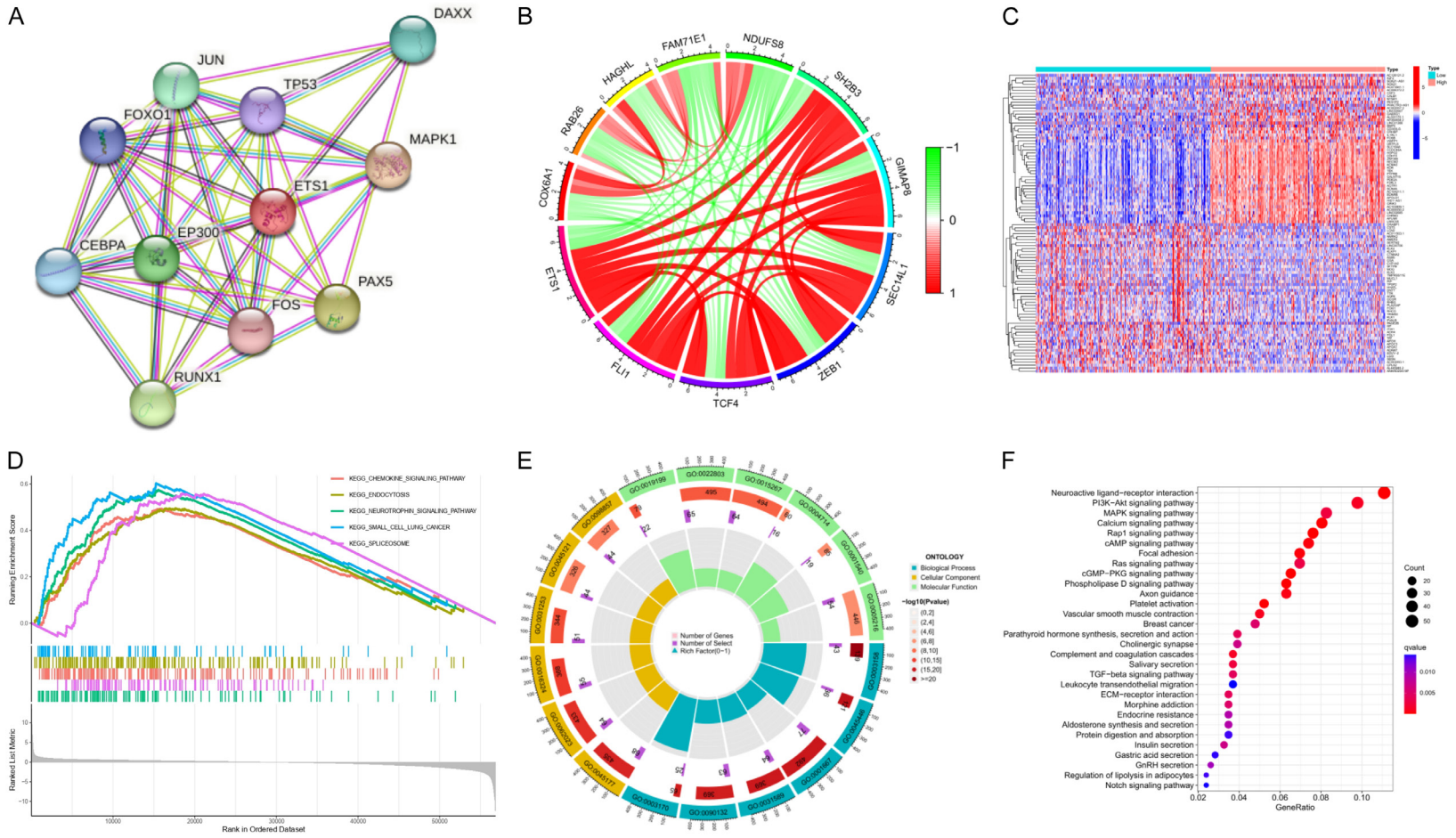

Figure 8. Related co-expressed and functional enrichment analysis of ETS1 in ccRCC. A. PPI networks and functional enrichment analyses; B. Circus analysis of overlapping genes expression in ccRCC; C. Co-expression of ETS1 and related genes in ccRCC; D. Enrichment plots of GSEA in ccRCC with a high ETS1 expression phenotype; E. Circus plot of GO pathway associated with ETS1 expression; F. KEGG pathway associated with ETS1 expression. ccRCC, Clear cell renal cell carcinoma.

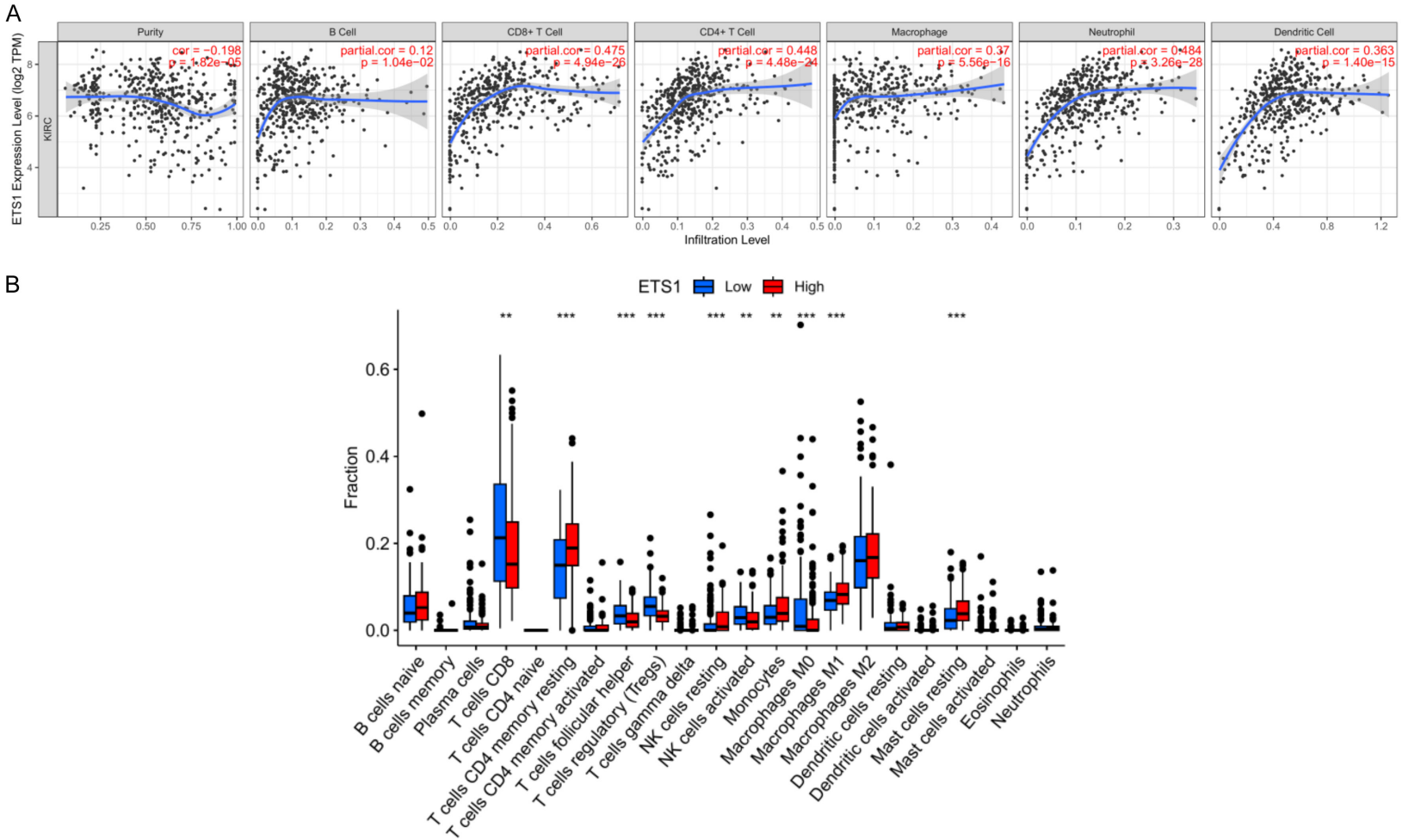
A
Purity
B Cell
CD8+ T Cell
CD4+ T Cell
Macrophage
Neutrophil
Dendritic Cell
cor = −0.198
p = 1.82e−05
partial.cor = 0.12
p = 1.04e−02
partial.cor = 0.475
p = 4.94e−26
partial.cor = 0.448
p = 4.48e−24
partial.cor = 0.37
p = 5.56e−16
partial.cor = 0.484
p = 3.26e−28
partial.cor = 0.363
p = 1.40e−15
KIRC
ETS1 Expression Level (log2 TPM)
Infiltration Level
B
ETS1 Low High
Fraction
B cells naive
B cells memory
Plasma cells
T cells CD8
T cells CD4 naive
T cells CD4 memory resting
T cells CD4 memory activated
T cells follicular helper
T cells regulatory (Tregs)
T cells gamma delta
NK cells resting
NK cells activated
Monocytes
Macrophages M0
Macrophages M1
Macrophages M2
Dendritic cells resting
Dendritic cells activated
Mast cells resting
Mast cells activated
Eosinophils
Neutrophils

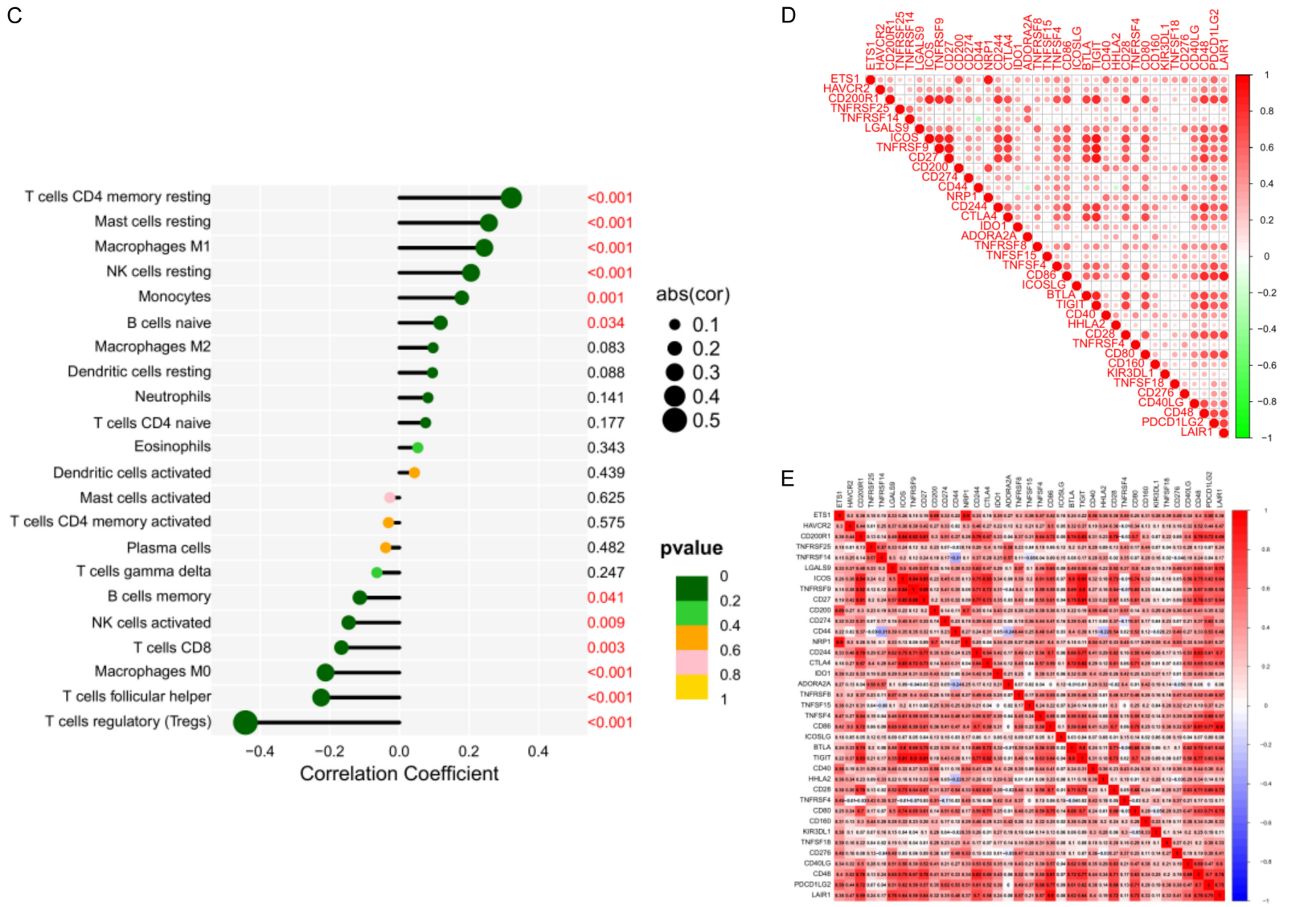

Figure 9. Association analysis of ETS1 gene expression and immune infiltration. A. Relationship between ETS1 and tumor immune infiltration in ccRCC; B. Relationship between high and low expression of ETS1 and the level of immune cell infiltration; C. Association analysis between ETS1 expression and immune cells; D. Correlations between ETS1 and various immune cells and immune checkpoints; E. Co-expression of ETS1 and immune-related genes in ccRCC. ccRCC, Clear cell renal cell carcinoma.

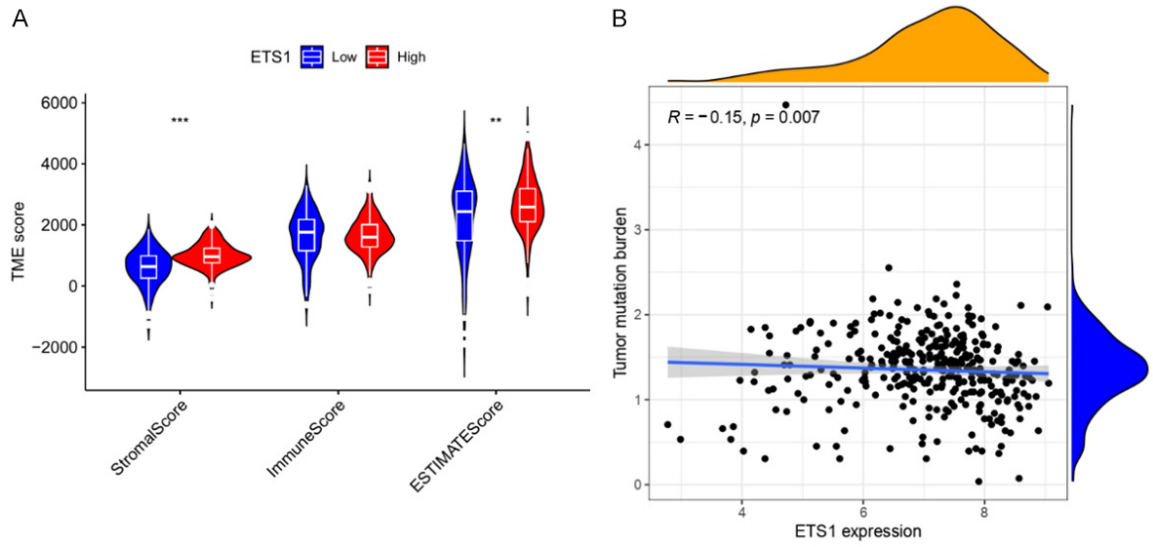

Figure 10. Analysis of ETS1 with tumor microenvironment and tumor mutation burden in ccRCC. A. Relationship between ETS1 and tumor microenvironment in ccRCC; B. Association between expression of ETS1 and TMB. $^{*}P < 0.05$, $^{***}P < 0.001$. RCC, Renal cell carcinoma.

Cox hazard regression analysis, indicating that ETS1 could serve as an independent prognostic factor in ccRCC.

To confirm the protein expression of ETS1, a CPTAC analysis demonstrated that ETS1 had a higher expression in primary ccRCC tumors than normal kidney tissues, consistent with its mRNA expression levels. As protein phosphorylation has been shown to play critical roles in multiple cancers, we also analyzed the expression of ETS1 phosphoprotein and found that it was highly expressed in primary ccRCC tumors compared to normal tissues at the S26 phosphorylation sites [34, 35]. A previous study demonstrated that phosphorylation of ETS1 at threonine 265 and serine 269 promoted protein stability, induced the transcriptional activation of matrix metalloproteinase (MMP)-9, and increased cell migration [36]. Several researchers have used GSEA to identify ETS1-related signaling pathways [37]. Ultimately, two eligible signaling pathways, including the Huntington's disease pathway and the ECM (extracellular matrix)-associated pathway, showed significant enrichment in the high-ETS1 expression phenotype. All of these identified signaling pathways helped us better understand the pathophysiologic mechanisms of ccRCC. In this article, we created a nomogram that used ETS1 and six clinical parameters to intuitively estimate OS probabilities in ccRCC. As a result, the C-index, 1-, 3-, and 5-year AUCs, and calibration curves indicated that this nomogram had moderate predictive accuracy and satisfactory performance.

We delved deeper into the possible correlations between ETS1 and immunity, with a focus on four areas: tumor microenvironment, tumor immune infiltration, immune cell pathways, and immune checkpoint molecules. As prior literature suggests, both the tumor microenvironment and tumor immune infiltration can impact the prognosis of ccRCC and its response to immunotherapy. Additionally, numerous genes have been found to have significant associations with immune cell pathways and checkpoint molecules [38-40]. As for tumor immune infiltration, ETS1 was significantly associated with B Cells, CD8+ T Cells, CD4+ T cells, macrophages, neutrophils, and dendritic cell infiltration. ETS1 has strongly profound effects on B cells, T cells, and NK cells, each of which has high levels expression of ETS1 under normal physiologic conditions [10]. Several T cell lineage issues observed in ETS1 knockout mice include anomalous thymic differentiation, reduced peripheral T cell counts, decreased production of IL-2, a shift towards a memory/effector phenotype, and decreased production of Th1 and Th2 cytokines [41]. Recently, it was shown that ETS1 is crucial for maintaining the expression of CD127 (IL7Rα) in peripheral T

cells [42]. In addition, ETS1 is also expressed in CD8 T cells so that mice lacking Ets1 have deficiencies in CD8 T cell development and function [43, 44].

In relation to the tumor microenvironment, ETS1 demonstrated significant associations with the StromalScore and ESTIMATEScore. Analysis of ETS1 co-expression with immune checkpoint molecules or immune cell pathways revealed significant correlations between ETS1 and the CD8+ T cellss, neutrophils, dendritic cells, natural killer T cells, and CD56dim cell pathways in ccRCC using data from the TCGA dataset. According to multiple studies, the expression of ETS1 is mainly restricted to immune tissues, such as the thymus, spleen, and lymph nodes, in adult mice under normal conditions [45]. Similar patterns are shown in adult humans, where high expression of ETS1 is found mainly in lymphoid tissues [46]. Ets1 is expressed in B cells, T cells, NK cells, and NK T cells and is also induced in other non-lymphoid cell types by response to certain stimuli [47, 48]. Above all, these indicated that ETS1 was closely connected to immunity in ccRCC. Due to the high mutation load of a tumor, patients with TMB-High produce many antigens in the body and have a more adequate response to immunotherapy, with greater clinical benefits. As can be seen from our analysis, TMB in the low expression group was significantly higher than that in the high expression group, which further emphasized the correlation between the ETS1 gene and immunity. How to screen out patients who can benefit from the massive number of patients is particularly important. TMB is an emerging biomarker for the prediction of immune efficacy [49].

Previous investigations also found that it was hypothesized to prevent the progression of ccRCC by repressing the expression of ETS1 [50]. A previous study indicated that SBF2-AS1 promoted the growth and advancement of ccRCC by suppressing miR-338-3p and increasing ETS1 expression [51]. To our knowledge, SBF2-AS1 increased miR338-3p-targeted ETS1 in ccRCC cells to promote cell proliferation, migration and invasion while inhibiting apoptosis [51]. Upregulated miR-338-3p could give rise to a reduction in the invasiveness of RCC cells, which indicated that it may act as a tumor suppressor in RCC [52]. As a result, SBF2-AS1 could regulate the biologic activities of ccRCC by targeting ETS1. In summary, increased ETS1 expression in tumors is an independent predictor of favorable prognosis in ccRCC [15].

Our analysis shares common limitations with similar retrospective studies. First, due to the nature of our study, clinical information from TCGA was limited, and some critical data could not be obtained. Secondly, additional in vitro and in vivo experiments should be designed to further elucidate the detailed mechanism by which ETS1 affects the immune infiltration of ccRCC. Although these studies have provided a clearer understanding of ETS1 function, many unanswered questions remain regarding ETS1 structure, regulation, and biologic function.

Despite these limitations, our study has several strengths. We not only analyzed ETS1 mRNA expression by qRT-PCR validation, but also verified its protein expression by CPTAC analysis and the HPA database, making our results more persuasive. Additionally, we analyzed multiple aspects of ETS1 in ccRCC, including mutation features, nomogram, protein-protein interaction, tumor immune infiltration, immune cell pathways, and checkpoint molecules. The recent advances in understanding molecular discoveries in ccRCC should facilitate the development of novel and highly effective therapies.

Conclusions

ccRCC tissue had higher levels of ETS1 than normal tissue. High ETS1 expression correlates with earlier clinical stage and better prognosis in ccRCC and may develop into a biomarker for the prognosis of ccRCC. The findings may help us obtain deeper insight into therapeutic targeting of ccRCC.

Acknowledgements

We would like to thank Editage for the language editing provided for this manuscript. This work was supported by Zhouzheng prestigious Chinese physician Inheritance Studio.

Disclosure of conflict of interest

None.

Address correspondence to: Yanna Yu, The First Affiliated Hospital of Guangzhou University of Chinese Medicine, Guangzhou, Guangdong, China. E-mail: yuyanna2023@163.com; Zheng Zhou, Dongguan Hospital of Guangzhou University of Chinese Medicine, Dongguan, Guangdong, China. E-mail: zhengz1107@163.com

References

[1] Siegel RL, Miller KD, Fuchs HE and Jemal A. Cancer statistics, 2021. CA Cancer J Clin 2021; 71: 7-33.

[2] Ricketts CJ, Crooks DR, Sourbier C, Schmidt LS, Srinivasan R and Linehan WM. SnapShot: renal cell carcinoma. Cancer Cell 2016; 29: 610-610, e1.

[3] Choueiri TK and Motzer RJ. Systemic therapy for metastatic renal-cell carcinoma. N Engl J Med 2017; 376: 354-366.

[4] Motzer RJ, Jonasch E, Agarwal N, Bhayani S, Bro WP, Chang SS, Choueiri TK, Costello BA, Derweesh IH, Fishman M, Gallagher TH, Gore JL, Hancock SL, Harrison MR, Kim W, Kyriakopoulos C, LaGrange C, Lam ET, Lau C, Michaelson MD, Olencki T, Pierorazio PM, Plimack ER, Redman BG, Shuch B, Somer B, Sonpavde G, Sosman J, Dwyer M and Kumar R. Kidney cancer, version 2.2017, NCCN clinical practice guidelines in oncology. J Natl Compr Canc Netw 2017; 15: 804-834.

[5] Kang HW, Kim SM, Kim WT, Yun SJ, Lee SC, Kim WJ, Hwang EC, Kang SH, Hong SH, Chung J, Kwon TG, Kim HH, Kwak C, Byun SS and Kim YJ; KORCC (KOrean Renal Cell Carcinoma) Group. The age-adjusted Charlson comorbidity index as a predictor of overall survival of surgically treated non-metastatic clear cell renal cell carcinoma. J Cancer Res Clin Oncol 2020; 146: 187-196.

[6] Seth A and Watson DK. ETS transcription factors and their emerging roles in human cancer. Eur J Cancer 2005; 41: 2462-2478.

[7] Findlay VJ, LaRue AC, Turner DP, Watson PM and Watson DK. Understanding the role of ETS-mediated gene regulation in complex biological processes. Adv Cancer Res 2013; 119: 1-61.

[8] Wang C, Kam RK, Shi W, Xia Y, Chen X, Cao Y, Sun J, Du Y, Lu G, Chen Z, Chan WY, Chan SO, Deng Y and Zhao H. The proto-oncogene transcription factor Ets1 regulates neural crest development through histone deacetylase 1 to mediate output of bone morphogenetic protein signaling. J Biol Chem 2015; 290: 21925-21938.

[9] Dong Z. Acetylation of Ets-1 is the key to chromatin remodeling for miR-192 expression. Sci Signal 2013; 6: pe21.

[10] Garrett-Sinha LA. Review of Ets1 structure, function, and roles in immunity. Cell Mol Life Sci 2013; 70: 3375-3390.

[11] Dejana E, Taddei A and Randi AM. Foxs and Ets in the transcriptional regulation of endothelial cell differentiation and angiogenesis. Biochim Biophys Acta 2007; 1775: 298-312.

[12] Li YH, Lv MF, Lu MS and Bi JP. Bone marrow mesenchymal stem cell-derived exosomal MiR-338-3p represses progression of hepatocellular carcinoma by targeting ETS1. J Biol Regul Homeost Agents 2021; 35: 617-627.

[13] Teng Y, Cang B, Mao F, Chen W, Cheng P, Peng L, Luo P, Lu D, You N, Zou Q and Zhuang Y. Expression of ETS1 in gastric epithelial cells positively regulate inflammatory response in Helicobacter pylori-associated gastritis. Cell Death Dis 2020; 11: 498.

[14] Suzuki H, Romano-Spica V, Papas TS and Bhat NK. ETS1 suppresses tumorigenicity of human colon cancer cells. Proc Natl Acad Sci U S A 1995; 92: 4442-4446.

[15] Tan X, Zheng S, Liu W, Liu Y, Kang Z, Li Z, Li P, Song J, Hou J, Yang B, Han X, Wang F, Jing C and Cao G. Effect of APOBEC3A functional polymorphism on renal cell carcinoma is influenced by tumor necrosis factor-α and transcriptional repressor ETS1. Am J Cancer Res 2021; 11: 4347-4363.

[16] Li S, Yan G, Yue M, Kang Z and Wang L. MicroRNA-766 inhibits the malignant biological behaviours of pancreatic ductal adenocarcinoma by directly targeting ETS1. Mol Med Rep 2019; 19: 1380-1387.

[17] Chen C, Xue S, Zhang J, Chen W, Gong D, Zheng J, Ma J, Xue W, Chen Y, Zhai W and Zheng J. DNA-methylation-mediated repression of miR-766-3p promotes cell proliferation via targeting SF2 expression in renal cell carcinoma. Int J Cancer 2017; 141: 1867-1878.

[18] Wang Z, Jensen MA and Zenklusen JC. A practical guide to the cancer genome atlas (TCGA). Methods Mol Biol 2016; 1418: 111-141.

[19] Robin X, Turck N, Hainard A, Tiberti N, Lisacek F, Sanchez JC and Müller M. pROC: an open-source package for R and S+ to analyze and compare ROC curves. BMC Bioinformatics 2011; 12: 77.

[20] Ellis MJ, Gillette M, Carr SA, Paulovich AG, Smith RD, Rodland KK, Townsend RR, Kinsinger C, Mesri M, Rodriguez H and Liebler DC; Clinical Proteomic Tumor Analysis Consortium (CPTAC). Connecting genomic alterations to cancer biology with proteomics: the NCI Clinical Proteomic Tumor Analysis Consortium. Cancer Discov 2013; 3: 1108-1112.

[21] Uhlén M, Fagerberg L, Hallström BM, Lindskog C, Oksvold P, Mardinoglu A, Sivertsson Å, Kampf C, Sjöstedt E, Asplund A, Olsson I,

Edlund K, Lundberg E, Navani S, Szigyarto CA, Odeberg J, Djureinovic D, Takanen JO, Hober S, Alm T, Edqvist PH, Berling H, Tegel H, Mulder J, Rockberg J, Nilsson P, Schwenk JM, Hamsten M, von Feilitzen K, Forsberg M, Persson L, Johansson F, Zwahlen M, von Heijne G, Nielsen J and Pontén F. Proteomics. Tissue-based map of the human proteome. Science 2015; 347: 1260419.

[22] Chen F, Chandrashekar DS, Varambally S and Creighton CJ. Pan-cancer molecular subtypes revealed by mass-spectrometry-based proteomic characterization of more than 500 human cancers. Nat Commun 2019; 10: 5679.

[23] Chandrashekar DS, Bashel B, Balasubramanya SAH, Creighton CJ, Ponce-Rodriguez I, Chakravarthi BVSK and Varambally S. UALCAN: a portal for facilitating tumor subgroup gene expression and survival analyses. Neoplasia 2017; 19: 649-658.

[24] Subramanian A, Tamayo P, Mootha VK, Mukherjee S, Ebert BL, Gillette MA, Paulovich A, Pomeroy SL, Golub TR, Lander ES and Mesirov JP. Gene set enrichment analysis: a knowledge-based approach for interpreting genome-wide expression profiles. Proc Natl Acad Sci U S A 2005; 102: 15545-15550.

[25] Ashburner M, Ball CA, Blake JA, Botstein D, Butler H, Cherry JM, Davis AP, Dolinski K, Dwight SS, Eppig JT, Harris MA, Hill DP, Issel-Tarver L, Kasarskis A, Lewis S, Matese JC, Richardson JE, Ringwald M, Rubin GM and Sherlock G. Gene ontology: tool for the unification of biology. The Gene Ontology Consortium. Nat Genet 2000; 25: 25-29.

[26] Kanehisa M, Sato Y, Kawashima M, Furumichi M and Tanabe M. KEGG as a reference resource for gene and protein annotation. Nucleic Acids Res 2016; 44: D457-462.

[27] de Barrios O, Galaras A, Trincado JL, Azagra A, Collazo O, Meler A, Agraz-Doblas A, Bueno C, Ballerini P, Cazzaniga G, Stam RW, Varela I, De Lorenzo P, Valsecchi MG, Hatzis P, Menéndez P and Parra M. HDAC7 is a major contributor in the pathogenesis of infant t(4;11) proB acute lymphoblastic leukemia. Leukemia 2021; 35: 2086-2091.

[28] Yoshihara K, Shahmoradgoli M, Martínez E, Vegesna R, Kim H, Torres-Garcia W, Treviño V, Shen H, Laird PW, Levine DA, Carter SL, Getz G, Stemke-Hale K, Mills GB and Verhaak RG. Inferring tumour purity and stromal and immune cell admixture from expression data. Nat Commun 2013; 4: 2612.

[29] Newman AM, Liu CL, Green MR, Gentles AJ, Feng W, Xu Y, Hoang CD, Diehn M and Alizadeh AA. Robust enumeration of cell subsets from tissue expression profiles. Nat Methods 2015; 12: 453-457.

[30] Wilson LA, Yamamoto H and Singh G. Role of the transcription factor Ets-1 in cisplatin resistance. Mol Cancer Ther 2004; 3: 823-832.

[31] Dittmer J. The role of the transcription factor Ets1 in carcinoma. Semin Cancer Biol 2015; 35: 20-38.

[32] Puzovic V, Brcic I, Ranogajec I and Jakic-Razumovic J. Prognostic values of ETS-1, MMP-2 and MMP-9 expression and co-expression in breast cancer patients. Neoplasma 2014; 61: 439-446.

[33] Peng C, Gao H, Niu Z, Wang B, Tan Z, Niu W, Liu E, Wang J, Sun J, Shahbaz M, Agrez M and Niu J. Integrin αvβ6 and transcriptional factor Ets-1 act as prognostic indicators in colorectal cancer. Cell Biosci 2014; 4: 53.

[34] Motolani A, Martin M, Sun M and Lu T. Phosphorylation of the regulators, a complex facet of NF-κB signaling in cancer. Biomolecules 2020; 11: 15.

[35] Taddei ML, Pardella E, Pranzini E, Raugei G and Paoli P. Role of tyrosine phosphorylation in modulating cancer cell metabolism. Biochim Biophys Acta Rev Cancer 2020; 1874: 188442.

[36] Tsai CL, Jung SM, Chi LM, Tsai CN, Lin CY, Chao A and Lee YS. Glycogen synthase kinase-3 beta (GSK3β)-mediated phosphorylation of ETS1 promotes progression of ovarian carcinoma. Aging (Albany NY) 2021; 13: 13739-13763.

[37] Ma S, Zhou B, Yang Q, Pan Y, Yang W, Freedland SJ, Ding LW, Freeman MR, Breunig JJ, Bhowmick NA, Pan J, Koeffler HP and Lin DC. A transcriptional regulatory loop of master regulator transcription factors, PPARG, and fatty acid synthesis promotes esophageal adenocarcinoma. Cancer Res 2021; 81: 1216-1229.

[38] Pan Q, Wang L, Chai S, Zhang H and Li B. The immune infiltration in clear cell renal cell carcinoma and their clinical implications: a study based on TCGA and GEO databases. J Cancer 2020; 11: 3207-3215.

[39] Şenbabaoğlu Y, Gejman RS, Winer AG, Liu M, Van Allen EM, de Velasco G, Miao D, Ostrovnaya I, Drill E, Luna A, Weinhold N, Lee W, Manley BJ, Khalil DN, Kaffenberger SD, Chen Y, Danilova L, Voss MH, Coleman JA, Russo P, Reuter VE, Chan TA, Cheng EH, Scheinberg DA, Li MO, Choueiri TK, Hsieh JJ, Sander C and Hakimi AA. Tumor immune microenvironment characterization in clear cell renal cell carcinoma identifies prognostic and immunotherapeutically relevant messenger RNA signatures. Genome Biol 2016; 17: 231.

[40] Chen YN, Hou SQ, Jiang R, Sun JL, Cheng CD and Qian ZR. EZH2 is a potential prognostic predictor of glioma. J Cell Mol Med 2021; 25: 925-936.

[41] Bories JC, Willerford DM, Grévin D, Davidson L, Camus A, Martin P, Stéhelin D and Alt FW. Increased T-cell apoptosis and terminal B-cell differentiation induced by inactivation of the Ets-1 proto-oncogene. Nature 1995; 377: 635-638.
[42] Grenningloh R, Tai TS, Frahm N, Hongo TC, Chicoine AT, Brander C, Kaufmann DE and Ho IC. Ets-1 maintains IL-7 receptor expression in peripheral T cells. J Immunol 2011; 186: 969-976.
[43] Anderson MK, Hernandez-Hoyos G, Diamond RA and Rothenberg EV. Precise developmental regulation of Ets family transcription factors during specification and commitment to the T cell lineage. Development 1999; 126: 3131-3148.
[44] Bhat NK, Komschlies KL, Fujiwara S, Fisher RJ, Mathieson BJ, Gregorio TA, Young HA, Kasik JW, Ozato K and Papas TS. Expression of ets genes in mouse thymocyte subsets and T cells. J Immunol 1989; 142: 672-678.
[45] Maroulakou IG and Bowe DB. Expression and function of Ets transcription factors in mammalian development: a regulatory network. Oncogene 2000; 19: 6432-6442.
[46] Sacchi N, de Klein A, Showalter SD, Bigi G and Papas TS. High expression of ets-1 gene in human thymocytes and immature T leukemic cells. Leukemia 1988; 2: 12-18.
[47] Fisher CL, Ghysdael J and Cambier JC. Ligation of membrane Ig leads to calcium-mediated phosphorylation of the proto-oncogene product, Ets-1. J Immunol 1991; 146: 1743-1749.
[48] Chen JH. The proto-oncogene c-ets is preferentially expressed in lymphoid cells. Mol Cell Biol 1985; 5: 2993-3000.
[49] Huang Z, Yang J, Qiu W, Huang J, Chen Z, Han Y and Ye C. HAUS5 is a potential prognostic biomarker with functional significance in breast cancer. Front Oncol 2022; 12: 829777.
[50] Zhang L, Yan R, Zhang SN, Zhang HZ, Ruan XJ, Cao Z and Gu XZ. MicroRNA-338-3p inhibits the progression of bladder cancer through regulating ETS1 expression. Eur Rev Med Pharmacol Sci 2019; 23: 1986-1995.
[51] Yang X, Zhang Y and Fan H. Downregulation of SBF2-AS1 functions as a tumor suppressor in clear cell renal cell carcinoma by inhibiting miR-338-3p-targeted ETS1. Cancer Gene Ther 2021; 28: 813-827.
[52] Zhang X, Wang C, Li H, Niu X, Liu X, Pei D, Guo X, Xu X and Li Y. miR-338-3p inhibits the invasion of renal cell carcinoma by downregulation of ALK5. Oncotarget 2017; 8: 64106-64113.